

Quasi One-Dimensional Spin Fluctuations in $\text{YBa}_2\text{Cu}_3\text{O}_{6+x}$

D. N. Aristov^{1,2} and D. R. Grempel¹

¹*CEA/Département de Recherche Fondamentale sur la Matière Condensée
SPSMS/MDN, CENG, 17, rue des Martyrs, 38054 Grenoble Cedex 9, France*

²*Petersburg Nuclear Physics Institute, 188350 Gatchina, Saint-Petersburg, Russia*

(March 31, 2018)

Abstract

We study the spin fluctuation of the oxygen deficient planes of $\text{YBa}_2\text{Cu}_3\text{O}_{6+x}$. The Cu-O chains that constitute these planes are described by a model that includes antiferromagnetic interactions between spins and Kondo-like scattering of oxygen holes. The spectrum of magnetic excitations shows the presence of incommensurate dynamic fluctuations along the direction of the chains. The presence of itinerant holes is responsible for the existence of important differences between the spin dynamics of this system and that of a quasi-one-dimensional localized antiferromagnet. We comment on the possibility of experimental observation of these fluctuations.

PACS numbers: 75.10.Jm, 75.40.Gb, 74.72.Bk, 61.12.Ex

I. INTRODUCTION

A considerable amount of experimental and theoretical research has recently been consecrated to the study of the structural and electronic properties of the oxygen deficient (or CuO_x) planes of superconductors of the $\text{YBa}_2\text{Cu}_3\text{O}_{6+x}$ -type. It has been known for some time that these planes play an important role in the superconductivity of the YBCO compounds by regulating the hole concentration in the CuO_2 planes [1]. There is now evidence that they also have an interesting physics of their own [2,3]. The basic components of the CuO_x planes are $\text{Cu}_{n+1}\text{O}_n$ chain fragments in which Cu and O atoms form a linear alternating chain. Under stoichiometric conditions, $x = 0.5$ and $x = 1$, all chains are (ideally) infinitely long. Away from stoichiometry the length of the chains follows a certain distribution determined by x and the temperature but the physical properties of the chain planes are dominated by the longest chain fragments [4,5]. Band structure calculations [6,7] for $\text{YBa}_2\text{Cu}_3\text{O}_7$ show that the dispersion of the chain-derived bands which cross the Fermi level in the directions perpendicular to the chains is much weaker than that in the direction of the chains. This suggests that, to a first approximation, the latter may be viewed as decoupled from each other and from the CuO_2 planes. If this is correct, important $1-d$ fluctuation effects are expected in the charge and spin excitation spectra of the CuO_x planes. A recent inelastic neutron scattering study [2] of a $\text{YBa}_2\text{Cu}_3\text{O}_{6.93}$ crystal shows that such effects are indeed visible in the phonon spectrum of the chain planes. Their signature is the presence of purely inelastic satellites around the structural Bragg peaks at positions that correspond closely to the value of $2k_F$ for the one-dimensional chains predicted by the band structure calculations [7].

In this work we study the spin fluctuation spectrum of long $\text{Cu}_{n+1}\text{O}_n$ chains in the framework of a one-dimensional model of strongly interacting fermions. Most of the paper deals with the $T = 0$ case but we briefly discuss the extension of our calculations to finite temperatures in the concluding Section. Our main results are the following. The spin-spin correlation function of the chains is given by the convolution of two functions. One is the

dynamic structure factor of a one-dimensional Heisenberg antiferromagnet on a fictitious lattice that contains a number of sites equal to the total number of holes in the chain. This factor describes the part of the dynamic that results from the exchange interactions between the spins in the chain. The second factor, related to the density-density correlation function of the itinerant oxygen holes, takes into account the perturbation of the spin configurations that arise from the motion of the latter. The magnetic intensity is modulated along the direction of the chains [8] and is peaked at an incommensurate position, $Q_{max} = \pi(1 + c)$, where c is the nominal oxygen hole concentration in the chains (see below). The lineshape of the energy-integrated peak, very asymmetric, is quite different from that obtained for a one-dimensional Heisenberg antiferromagnet. The intensity at Q_{max} is distributed over an energy range given by the Fermi energy of the holes. However, enough intensity remains at low energies that observation of these excitations by inelastic neutron scattering might be feasible.

The organization of the rest of the paper is as follows. The model used to describe the Cu-O chains is presented in Section II. The calculation of the ground state spin-spin correlation function is described in III. In Section IV we discuss our results and their connection with experiment.

II. THE MODEL.

The simplest microscopic model for the Cu-O chains is the 1- d Emery Hamiltonian [9] defined by:

$$H = -t \sum_{\langle r, \rho \rangle} \sum_{\sigma} (p_{r\sigma}^{\dagger} d_{\rho\sigma} + d_{\rho\sigma}^{\dagger} p_{r\sigma}) + \sum_r (\epsilon_p n_r + U_p n_{r\uparrow} n_{r\downarrow}) + \sum_{\rho} (\epsilon_d n_{\rho} + U_d n_{\rho\uparrow} n_{\rho\downarrow}), \quad (1)$$

Here, r and ρ denote the O and Cu sites, respectively, d_{σ} and p_{σ} are annihilation operators for holes of spin σ on Cu and O sites, the occupation number of a hole with spin σ is n_{σ} and $n = \sum_{\sigma} n_{\sigma}$. Hopping is only allowed between nearest neighbors. The values of the charge transfer gap and of the on-site Coulomb repulsion appropriate for the description of the

CuO chains are [10] $(\epsilon_p - \epsilon_d) = 2t$, and $U_d = 2U_p = 8t$, where $t \approx 1eV$ is the Cu-O transfer integral. In the following we shall measure energies from the position of the Cu level and set $\epsilon_d = 0$.

An additional parameter, the charge of the fragment, has to be fixed in order to completely define the problem. Taking the Cu^{+1} and O^{-2} configurations as reference states, one may easily see [1] that a neutral fragment with N Cu atoms contains $2N - 1$ holes. However, because of the transfer of charge between the CuO_x and the CuO_2 planes the number of holes in the chains, $N(1 + c)$ with $0 \leq c \leq 1$, deviates from this value [10]. In a naive picture in which all the Cu ions in the chain are in the Cu^{2+} state, c is simply the concentration of oxygen holes. It is experimentally known [11] that the hole concentration in long chain fragments is $\nu_h \approx 1.3$. Therefore, for the systems discussed here, $c \approx 0.3$. It is however interesting to treat c as a free parameter and study the dependence on concentration of different physical quantities.

The Emery Hamiltonian of Eq. 1 gives a good a description of the static electronic properties of the chain fragments [10,12] but it can only be properly treated with numerical methods such as Quantum Monte Carlo or exact diagonalization that are not well suited for the calculation of the dynamic susceptibility. There is a limiting case, $U_d/t \rightarrow \infty$, ϵ_p/t and U_p/t finite but large, in which a more tractable model [13] can be derived from Eq. 1. In this limit the Cu occupation n_p is unity and charge fluctuations on the Cu sites only appear in virtual processes generated in perturbation theory by the kinetic energy term. In the 2nd order in t we generate a process in which an O hole hops from a site r to an adjacent O site, $r \pm 2$ leaving the spin *sequence* in the lattice unchanged [14]. This process, whose amplitude is $\tau = t^2/\epsilon_p$, is described by a tight-binding model for *spinless* free fermions defined on the oxygen sublattice:

$$H_1 = -\tau \sum_{j=1}^N (c_{j+1+1/2}^\dagger c_{j+1/2} + h.c.). \quad (2)$$

In the same order in t there is an exchange interaction between a spin on an oxygen site and the spins on neighboring Cu sites with coupling $J = t^2/(\epsilon_p + U_p)$. Finally, if there is

no O hole on a site r the Cu spins on sites $r \pm 1$ still interact antiferromagnetically with a coupling constant that is of the fourth-order in t , $J' = 4t^4/(\epsilon_p^2(2\epsilon_p + U_p))$. The spin part of the interaction is thus described by a $1-d$ Heisenberg Hamiltonian given by :

$$H_2 = \sum_{i=1}^{N+N_h-1} J_{i,i+1} \boldsymbol{\sigma}_i \cdot \boldsymbol{\sigma}_{i+1}, \quad (3)$$

where $N_h \equiv Nc$ is the number of oxygen holes in the system, $N + N_h$ is the total number of spins in the system and $\boldsymbol{\sigma}_i$ are spin $1/2$ operators. The nearest-neighbor coupling $J_{i,i+1} = J$ or J' depending on whether $(i, i + 1)$ is a Cu-O or a Cu-Cu pair, respectively.

Since the couplings $J_{i,i+1}$ depend upon the instantaneous hole distribution, the spin and charge degrees of freedom of the system are coupled and the total Hamiltonian is not exactly solvable in general. However, in the special case $J'/J = 1$ an exact solution can be found. This is because if the exchange coupling is the same for all pairs of spins regardless of the charge configuration, the Hamiltonian becomes the sum of two independent terms each of which is exactly solvable. In the case of the Cu-O chains the ratio of couplings $J'/J \approx 0.75$ is not unity but, as shown elsewhere [10], their *static* magnetic correlations are quite accurately described by an effective homogeneous model. It seems therefore natural to try and use it to compute the time-dependent correlation functions as well. This is the approach that we follow in this paper.

The appropriate parametrization of the effective model may be determined variationally. If we construct a trial ground-state wave function as the product of separate wavefunctions for the spins and for the holes and then determine the individual components by minimizing the total energy of the system, we obtain the effective model

$$H_{eff} = -\tau \sum_{j=1}^N (c_{j+1+1/2}^\dagger c_{j+1/2} + \text{h.c.}) + J_{eff}(c) \sum_{i=1}^{N+N_h-1} \boldsymbol{\sigma}_i \cdot \boldsymbol{\sigma}_{i+1}. \quad (4)$$

where $J_{eff}(c) = J'(1 - c) + cJ$ and we have omitted an energy shift that can be absorbed in a redefinition of the chemical potential of the holes. We find $J_{eff}/\tau \approx 0.3$ for $c = 0.3$.

In spite of the simple form of H_{eff} the spin-spin correlation function,

$$\mathcal{S}(Q, \Omega) = \int_{-\infty}^{\infty} dt e^{i\Omega t} \langle \mathbf{S}_Q(t) \cdot \mathbf{S}_{-Q}(0) \rangle, \quad (5)$$

is non-trivial because the relationship between \mathbf{S}_i and σ_i is not simple [15]. The difference between the coordinates of a spin measured in the real and in the fictitious lattices is determined by the number of holes located to its left. In terms of σ_k , the Fourier transform of the spins on the fictitious lattice, we have:

$$\mathbf{S}_l = (N + N_h)^{-1/2} \sum_k \sigma_k \exp ik(l + \sum_{j=1}^{l-1} c_{j+1/2}^\dagger c_{j+1/2}), \quad (6)$$

for Cu sites, and

$$\mathbf{S}_{l+1/2} = (N + N_h)^{-1/2} \sum_k \sigma_k \exp ik(l + 1 + \sum_{j=1}^{l-1} c_{j+1/2}^\dagger c_{j+1/2}) c_{l+1/2}^\dagger c_{l+1/2}, \quad (7)$$

for O sites that only carry a spin when they are occupied by a hole.

Substituting Eqs. 6 and 7 in Eq. 5 and using the fact that the ground-state wavefunction of the decoupled Hamiltonian factorizes, $\mathcal{S}(Q, \Omega)$ may be written as a convolution :

$$\mathcal{S}(Q, \Omega) = \int_{-\pi}^{\pi} \frac{dk}{2\pi} \int_{-\infty}^{\infty} \frac{d\omega}{2\pi} |A(Q, k)|^2 f(k, \omega) \mathcal{C}_k(Q - \tilde{k}, \Omega - \omega), \quad (8)$$

where $\tilde{k} = k(1 + c)$.

The first factor in Eq. 8, $f(k, \omega)$, is the dynamic spin correlation function of the fictitious $1-d$ Heisenberg model of Eq. 3,

$$f(k, \omega) = \int_{-\infty}^{\infty} dt e^{i\omega t} \langle \sigma_k(t) \cdot \sigma_{-k}(0) \rangle_{H_2}. \quad (9)$$

The second factor, \mathcal{C}_k , describes the effects of the hole dynamics and is given by the space-time Fourier transform of :

$$\mathcal{C}_k(l, l'; t, t') = \left\langle \exp \left[ik \sum_{q \neq 0} \phi(q, l) \rho(q, t) \right] \exp \left[-ik \sum_{q \neq 0} \phi(q, l') \rho(q, t') \right] \right\rangle_{H_1}, \quad (10)$$

where the density operator is given by :

$$\rho(q) = N^{-1} \sum_p c_p^\dagger c_{p+q}, \quad (11)$$

and we have defined $\phi(l, q) = (1 - e^{iql})/(1 - e^{iq})$. The $q=0$ component of the density is not present in Eq. 10. Searate treatment of this component leads to the appearance of \tilde{k} instead of k in the argument of \mathcal{C}_k in Eq. 8. Finally, $A(Q, k)$ is a coherence factor given by

$$A(Q, k) = 1 + \frac{\sin(Q - k)/2}{\sin(k/2)}. \quad (12)$$

This factor takes into account the phase shift between Cu and O spins and it is derived in Appendix A.

III. EVALUATION OF THE CORRELATION FUNCTION.

The evaluation of the dynamic structure factor in Eq. 8 requires the knowledge of the individual correlation functions $f(k, \omega)$ and $\mathcal{C}_k(q, \omega)$. The dynamic correlation function of the one-dimensional Heisenberg antiferromagnet has been discussed in reference [16]. This function cannot be obtained in closed form but a very accurate approximate expression for it has been derived [16] using a combination of exact analytic and numerical results :

$$f(k, \omega) = 3a \theta(\omega) \theta(\pi J_{eff} \sin(|k|/2) - \omega) \left(\omega^2 - \left(\frac{\pi}{2} J_{eff} \sin k \right)^2 \right)^{-1/2}, \quad (13)$$

where $a = 1.4579$ is a numerical constant. There are no sharp spinwave excitations in the system but the spectral function is strongly peaked at the lower edge of the spectrum where the spectral weight diverges as $(\omega - \omega_s(k))^{-1/2}$ with $\omega_s(k) = \pi J_{eff}/2 \sin k$.

It will be seen below that most of the spectral weight in $\mathcal{S}(Q, \Omega)$ is concentrated in the neighborhood of $Q_{max} = \pi(1 + c) \pmod{2\pi}$. Since $f(k, \omega)$ is strongly peaked, the structure factor in the neighborhood of Q_{max} is determined by the long distance part of the fermionic correlator \mathcal{C}_k in Eq. 8. This part of the response is determined by the low energy excitations of the electron gas in which the momenta of excited particles and holes are all near $\pm k_F$, the Fermi momentum of the holes.

Eq. 10 may be evaluated using a well known procedure [17] in which the fermion density is split into contributions from right and left moving fermions with constant group-velocity. Since the fermionic Hamiltonian is particle-hole symmetrical it is sufficient to compute \mathcal{C}_k for $c \leq 1/2$ and make the transformation $c \rightarrow (1 - c)$ to obtain the corresponding expression for $c > 1/2$. We write

$$\rho(q) = \rho_+(q) + \rho_-(q) \equiv N^{-1} \sum_{p>0} c_p^\dagger c_{p+q} + N^{-1} \sum_{p<0} c_p^\dagger c_{p+q}, \quad (14)$$

and approximate the group velocity of right and left moving fermions by $\pm v_F$ respectively, where the Fermi velocity is $v_F = 2\tau \sin k_F$ and $k_F = \pi c$ ($k_F = \pi(1 - c)$ for $c > 1/2$). With this approximation the time dependence of the density operators becomes very simple, $\rho_\pm(q, t) = e^{\pm i\omega_q t} \rho_\pm(q)$ and $\omega_q = v_F |q|$.

The long wave-length density fluctuations of the $1-d$ electron gas may be represented by boson operators defined by the relations [19] :

$$\begin{aligned} \rho_+(q) &= v(q) \left(\theta(q) b_q^+ + \theta(-q) b_{-q} \right) \\ \rho_-(q) &= v(q) \left(\theta(q) b_{-q} + \theta(-q) b_q^+ \right), \end{aligned} \quad (15)$$

where $v(q) = \sqrt{|q|/(2N\pi)}$. With the definition

$$\mathcal{A}(l, t) \equiv \sum_q \phi(q, l) \rho(q, t) = \sum_q v(q) \phi(q, l) \left[e^{i\omega_q t} b_q^+ + e^{-i\omega_q t} b_{-q} \right], \quad (16)$$

we may rewrite Eq. 10 in the form :

$$\mathcal{C}_k(l, l'; t, t') = \langle \exp ik\mathcal{A}(l, t) \exp -ik\mathcal{A}(l', t') \rangle_{H_1} \quad (17)$$

The evaluation of this expression in Appendix B yields :

$$\mathcal{C}_k(l, l'; t, t') = \exp \left[-\frac{k^2}{4\pi^2} \mathcal{F}(l, l', t - t') \right], \quad (18)$$

where

$$\mathcal{F}(l, l'; t) = 4\pi^2 \sum_{|q| \leq k_F} v^2(q) \frac{e^{-i\omega_q t} (1 - \cos q(l - l')) + (1 - e^{-i\omega_q t}) (2 - \cos ql - \cos ql')}{2(1 - \cos q)}. \quad (19)$$

The integration over momenta in Eq. 19 is cutoff at $q \sim k_F$, the wave vector below which the density fluctuations of the electron gas can be treated as well defined excitations. In the thermodynamic limit ($l, l' \rightarrow \infty, |l - l'|$ finite) $\mathcal{F}(l, l'; t)$ depends on l and l' only through the difference ($l - l'$). Evaluating the integral over momentum in Eq. 19 in the logarithmic approximation we find :

$$\mathcal{C}_k(l; t) = \left[(1 + ik_F(l + v_F t))(1 - ik_F(l - v_F t))(1 + iE_F t)^2 \right]^{-\alpha_k}, \quad (20)$$

where $E_F = v_F k_F$ is the Fermi energy, and $\alpha_k = (k/2\pi)^2 \leq 1/4$.

The space-time Fourier transform of $\mathcal{C}_k(l; t)$ can be found analytically. For q in the first Brillouin zone :

$$\mathcal{C}_k(q, \omega) = \frac{4\pi^2 \theta(\omega) (2k_F)^{1-4\alpha_k} e^{-\omega/E_F}}{E_F \Gamma(\alpha_k) \Gamma(3\alpha_k) (\omega^2/v_F^2 - q^2)^{1-3\alpha_k} |q|^{2\alpha_k}} F(\alpha_k, 2\alpha_k - 1/2, 3\alpha_k; 1 - (\omega/qv_F)^2), \quad (21)$$

where F is the Gauss hypergeometric function. $\mathcal{C}_k(q, \omega)$ diverges at the lower end of the spectrum, at $\omega = |q|v_F$, the dispersion relation for density waves in the electron gas. At high energies the spectrum is cut off exponentially at $\omega \gtrsim E_F$.

The instantaneous correlation functions can be obtained by integrating Eqs. 13 and 21 over frequency. For the Heisenberg model the result is [16] :

$$f(k) = \frac{3a}{2\pi} \log \left| \frac{1 + \sin |k/2|}{\cos(k/2)} \right| \approx \frac{3a}{2\pi} \log \left| \frac{4}{\pi - |k|} \right|. \quad (22)$$

The approximate expression quoted on the right hand side of Eq. 22 derived near the zone boundary at $k = \pm\pi$ where $f(k)$ diverges logarithmically is in fact remarkably accurate over most of the Brillouin zone and will be used in our calculations below. The instantaneous value of the fermionic correlator is given by :

$$\mathcal{C}_k(q) = \frac{2^{1-\alpha_k} \sqrt{2\pi}}{\Gamma(\alpha_k) k_F} \left| \frac{q}{k_F} \right|^{-(1/2-\alpha_k)} K_{1/2-\alpha_k}(q/k_F). \quad (23)$$

$\mathcal{C}_k(q)$ is strongly peaked at $q = 0$ where it diverges as $\mathcal{C}_k(q) \approx q^{-(1-2\alpha_k)}$. Away from the center of the Brillouin zone $\mathcal{C}_k(q)$ decays exponentially, $\mathcal{C}_k(q) \approx \exp(-|q|/k_F)$.

The rapid decrease of $f(k, \omega)$ away from the zone boundary restricts the interval of the k -integration in Eq. 8 to the vicinity of $k = \pm\pi$. This allows us to linearize the bottom of the spectrum of the spin excitations writing $\omega_s(k) \approx \pi J_{eff}(\pi - |k|)/2$ and to replace the exponent α_k in Eq. 21 by $\alpha = 1/4$, its value at the zone boundary. With this approximation the fermionic correlator becomes :

$$\mathcal{C}_k(q, \omega) \approx \theta(\omega) \frac{4\pi \exp(-\omega/E_F)}{k_F \sqrt{2qv_F}} \frac{1}{(\omega^2 - q^2 v_F^2)^{1/4}} \equiv \mathcal{C}(q, \omega). \quad (24)$$

Carefully analyzing the contribution to the integral over k in Eq. 8 of the different regions where the spectral weights of f and \mathcal{C} are simultaneously large, and using the fact that the

structure factor varies smoothly compared to the two other factors in the integral, we may write the dynamic structure factor in the approximate form :

$$\mathcal{S}(Q, \Omega) = |A_+|^2 \Phi(Q - \pi(1 + c), \Omega) + |A_-|^2 \Phi(-Q + \pi(1 - c), \Omega), \quad (25)$$

where we have defined

$$\Phi(\kappa, \Omega) = 3a \int_0^\Omega \frac{d\omega e^{-\omega/E_F}}{v_s E_F (1 + c)} \int_\kappa^\infty \frac{dq}{\pi \sqrt{2|q|}} \left[\left(\frac{\Omega - \omega}{v_s} \right)^2 - |q - \kappa|^2 \right]^{-1/2} \left[\left(\frac{\omega}{v_F} \right)^2 - q^2 \right]^{-1/4}. \quad (26)$$

Here, $v_s = \pi J_{eff}/2(1 + c)$ is the renormalized spinwave velocity and the amplitudes A_\pm are given by

$$A_\pm = 1 \pm \sin \frac{\pi c}{2}. \quad (27)$$

Eq. 25 contains the main result of this work. The structure factor of the chains appears as the sum of two contributions. We will be seen below that $\Phi(\kappa, \Omega)$ peaks at $\kappa \sim 0$ and is exponentially small for $\kappa \geq 0$. Therefore, the first term is important for $Q \lesssim \pi(1 + c)$ and the second one for $Q \gtrsim \pi(1 - c)$. For vanishing hole concentration $A_\pm = 1$, and the two Φ functions reduce to the $Q \leq \pi$ and $Q \geq \pi$ parts of $f(Q, \Omega)$, respectively. For a finite hole concentration the corresponding peaks shift and broaden and the result is a distorted lineshape.

In order to make further progress we must analyze in detail the properties of $\Phi(\kappa, \Omega)$. We begin by examining the properties of the instantaneous function obtained by integrating Eq. 26 over frequency. The result can be expressed in terms of the convolution of the two static functions defined in Eqs. 22 and 23,

$$\Phi(\kappa) = \frac{3a}{2\pi(1 + c)} \int_\kappa^\infty \frac{dq}{2\pi} \mathcal{C}(q) \log \left| \frac{4(1 + c)}{q - \kappa} \right|, \quad (28)$$

where $\mathcal{C}(q) \equiv \mathcal{C}_\pi(q)$ (cf. Eq. 23) and we have used the asymptotic form of $f(k)$ given in Eq. 22.

For $c \rightarrow 0$ and $c \rightarrow 1$ where k_F vanishes, $\mathcal{C}(q) \rightarrow 2\pi\delta(q)$ and $\Phi(\kappa) \rightarrow 3a/(2\pi(1 + c))\theta(-\kappa) \log |4(1 + c)/\kappa|$. For intermediate values of the hole concentration $\Phi(\kappa)$ may be obtained analytically in two limits. At large $|\kappa/k_F|$ we find :

$$\Phi(\kappa) \sim \begin{cases} \frac{3a}{2\pi(1+c)} \log \left| \frac{4(1+c)}{\kappa} \right| & , \kappa \ll -k_F \\ \frac{3ak_F}{16\pi(1+c)^2} \frac{2^{1/4}}{\Gamma(1/4)} \left(\frac{\kappa}{k_F} \right)^{-3/4} e^{-\kappa/k_F} \left(\gamma - 1 + \log \left[\frac{4(1+c)}{k_F} \right] \right) & , \kappa \gg k_F \end{cases}, \quad (29)$$

where γ is the Euler constant. We thus recover the behavior of the pure system for large negative values of κ . The exponential tail that we find for large and positive κ results from the smearing of the unperturbed correlation function by the moving holes.

We can also evaluate analytically Eq. 28 for small κ/k_F . The result is :

$$\Phi(\kappa) \sim \begin{cases} \Phi(0) - \frac{6a}{(2\pi^3)^{1/2}(1+c)} \sqrt{\kappa/k_F} (1 + 1/2 \log |(1+c)/\kappa|) & , \kappa > 0 \\ \Phi(0) - \frac{6a}{(2\pi^3)^{1/2}(1+c)} \sqrt{|\kappa|/k_F} (\pi/2 - 1 - 1/2 \log |(1+c)/\kappa|) & , \kappa < 0 \end{cases}, \quad (30)$$

where $\Phi(0)$, the value at $\kappa = 0$, is

$$\Phi(0) = \frac{3a}{4\pi(1+c)} \left(\log \frac{4(1+c)}{k_F} + c_0 \right), \quad (31)$$

and $c_0 = \gamma + \pi/4 + 3/2 \log 2 \approx 2.4$. For a finite concentration of holes $\Phi(\kappa)$ has a cusp at $\kappa=0$, a less singular behavior than at $c = 0$ where it diverges logarithmically at $\kappa = 0$.

The two asymptotic forms, Eqs. 29 and 30, match smoothly at $\kappa \approx k_F$ as shown in Fig. 1 where we plot the κ -dependence of $\Phi(\kappa)$ for different hole concentrations.

We now turn to a discussion of the frequency dependence of the spectral function. The excitation spectrum of the pure model goes down to zero-energy only at $\kappa=0$. The same is true for a finite hole concentration. Putting $\kappa = 0$ in Eq. 26 and performing the integral we find :

$$\begin{aligned} \Phi(0, \Omega) &= \frac{1}{2E_f(1+c)} \int_0^{(1+v_s/v_F)^{-1}} \frac{dx}{1-x} \psi(x, \Omega) F(1/4, 1/2, 1, h^{-2}(x)) + \\ &+ \frac{1}{2k_F \sqrt{2\pi v_s v_F}} \frac{\Gamma(1/4)}{\Gamma(3/4)(1+c)} \int_{(1+v_s/v_F)^{-1}}^1 \frac{dx}{\sqrt{x(1-x)}} \psi(x, \Omega) F(1/4, 1/4, 3/4, h^2(x)), \end{aligned} \quad (32)$$

where we have defined the functions $\psi(x, \Omega) = \theta(x - 1 + \pi J_{eff}/\Omega) e^{-\Omega x/E_f}$, and $h(x) = (v_F/v_s)(1-x)/x$. Fig. 2 shows a plot of $\Phi(0, \Omega)$ as given by Eq. 32 for several hole concentrations and for $\tau/J_{eff} = 3$, a value consistent with our parametrization of the Emery model.

In the pure Heisenberg model the spectral weight, $\Phi(0, \Omega) \approx \Omega^{-1}$, diverges at zero frequency. This divergence is cutoff for finite c by the motion of the holes and the intensity at $\Omega = 0$ is now finite. The weight missing at low energies is transferred to the high energy end of the spectrum where an exponential tail, $\Phi(0, \Omega) \sim \exp(-\Omega/E_F)(\pi J_{eff}/\Omega)^{-1/2}$, extends beyond the energy $\Omega_{max} = \pi J_{eff}$ where the spectrum of the pure Heisenberg model has a sharp cutoff. Analysis of Eq. 26 for finite κ is more complicated. In this case the square roots present in the integrand of Eq. 26 impose the inequalities $v_F|q| \leq \omega \leq \Omega - v_s|q - \kappa|$ on the domain of integration. This condition can only be satisfied if $\Omega \geq \kappa \min(v_F, v_s)$, *i.e.*, there is a threshold in $\Phi(\kappa, \Omega)$. Let us first consider the case $v_F > v_s$. The bottom of the spinwave continuum starts at $\Omega = v_s|\kappa|$. Near the onset, for $\Delta\Omega \equiv \Omega - \Omega_{min} \ll \Omega$, only the neighborhood of $q=0$ contributes to the integral in Eq. 25. Making the change of variables $q = (\omega/v_F) \sin \theta$ the latter may be rewritten as :

$$\begin{aligned} \Phi(Q, \Omega) = & \int_0^\Omega \frac{d\omega \sqrt{2} e^{-\omega/E_f}}{E_f(1+c)2\pi} \int_{-\pi/2}^{\pi/2} \frac{d\theta}{\sqrt{|\tan \theta|}} \left(\Delta\Omega + 2\kappa v_s - \omega \left(1 + \frac{v_s}{v_F} \sin \theta\right) \right)^{-1/2} \\ & \times \left(\Delta\Omega - \omega \left(1 - \frac{v_s}{v_F} \sin \theta\right) \right)^{-1/2}. \end{aligned} \quad (33)$$

The first factor in the integral over θ is dominated by $2\kappa v_s \simeq \Omega \gg \Delta\Omega$ which allows us to approximate

$$\begin{aligned} \Phi(\kappa, \Omega) & \approx \int_0^\Omega \frac{d\omega e^{-\omega/E_f}}{E_f(1+c)2\pi\sqrt{\kappa v_s}} \int_{-\pi/2}^{\pi/2} \frac{d\theta}{\sqrt{|\tan \theta|}} \left(\Delta\Omega - \omega \left(1 - \frac{v_s}{v_F} \sin \theta\right) \right)^{-1/2} \\ & \simeq \frac{\sqrt{\Delta\Omega}}{E_f(1+c)\pi\sqrt{\kappa v_s}} \int_{-\pi/2}^{\pi/2} \frac{d\theta}{\sqrt{|\tan \theta|(1 - \frac{v_s}{v_F} \sin \theta)}}. \end{aligned} \quad (34)$$

The last integral can be done and we find the result

$$\Phi(\kappa, \Omega) \simeq 2 \left(\frac{\Delta\Omega}{2\kappa v_s} \right)^{1/2} \frac{(1 - v_s^2/v_F^2)^{-1/4}}{E_f(1+c)}. \quad (35)$$

In the case $v_s > v_F$, the bottom of the excitation spectrum is at $\Omega = v_F|\kappa|$, *i.e.*, below the spinwave continuum. The integral over q in Eq. 26 is now dominated by $q \approx \kappa$. The integration may be performed in a way similar to the previous one and the result is :

$$\Phi(\kappa, \Omega) \simeq \frac{4}{3} \left(\frac{\Delta\Omega}{2\kappa v_F} \right)^{3/4} \frac{(v_s^2/v_F^2 - 1)^{-1/2}}{E_f(1+c)} e^{-\kappa/k_f}, \quad (36)$$

The motion of the holes modifies substantially the low energy part of the excitation spectrum of the chains. For finite c , $\Phi(\kappa, \Omega)$ vanishes at threshold (cf. Eqs. 35 and 36) in contrast with the situation at $c = 0$ where the spectral weight has an inverse square root divergence at $\Omega = v_s|\kappa|$. For $c \approx 0$ and $c \approx 1$ where $v_F < v_s$, there are hole-like excitations below the spinwave continuum. However, their total weight is small because they are confined to the region $|q - \pi(1+c)| \lesssim k_F$ by the exponential factor in Eq. 36. Elsewhere in momentum space the spectrum is essentially that of the Heisenberg antiferromagnetic chain. At intermediate hole concentrations $v_F > v_s$ and the excitation spectrum starts at the spinwave continuum but there exist excitations with energies up to E_F that drain spectral weight from the region $\omega \lesssim J_{eff}$. The crossover between these two regimes takes place when $v_s = v_F$, which for our parametrization of the model yields a critical concentration $c_{crit} \approx \frac{1}{\pi} \sin^{-1}(\pi J'/4\tau) \simeq 0.06$.

IV. DISCUSSION

The natural tool for experimental investigation of the magnetic fluctuations described above is inelastic scattering of spin polarized neutrons. In this Section we will use our results to compute the differential cross-section for magnetic neutron scattering. The latter is related to the dynamic structure factor of Eq. 8 by the expression [22]

$$\frac{d\sigma(q, \omega)}{d\Omega_s d\omega} = \frac{2}{3} (r_0 \gamma)^2 \frac{k_f}{k_i} \mathcal{S}(q, \omega), \quad (37)$$

where $r_0 = e^2/mc^2$, and $\gamma = 1.57$ is the neutron's gyromagnetic ratio. The neutron's initial and final momenta are k_i and k_f , respectively, q is the momentum transfer in the direction parallel to the chain, ω is the neutron's energy loss and $d\Omega_s$ is the element of solid angle in the direction of the outgoing neutron.

The intensity scattered by a quasi one-dimensional object is uniformly distributed in a plane perpendicular to it. Therefore, the intensity at any particular point in q -space is very small and it is generally impossible to resolve the structure factor both in q and ω . Under typical experimental conditions what is measured is the cross-section integrated in

energy from 0 up to the incident neutron energy, ω_N . If the experiment is performed under quasielastic conditions (*i.e.*, if most of the spectral weight is at energies smaller than ω_N) we have

$$\frac{d\sigma(q)}{d\Omega_{\mathbf{q}}} = \frac{2}{3}(r_0\gamma)^2\mathcal{S}(q) = 194 \text{ mbarn } \mathcal{S}(q), \quad (38)$$

where it has been assumed that $\int_0^{\omega_N} d\omega \mathcal{S}(q, \omega) \approx \int_0^{\infty} d\omega \mathcal{S}(q, \omega) = \mathcal{S}(q)$.

Using the results of the preceding Section we may write

$$\mathcal{S}(q) = W_+\Phi(q - \pi(1 + c)) + W_-\Phi(-q + \pi(1 - c)). \quad (39)$$

where $W_{\pm} = A_{\pm}^2$, and $\Phi(\kappa)$ was defined in Eq. 28. Figure 3 shows the evolution of $\mathcal{S}(q)$ with doping. In the limiting cases $c=0$ and $c=1$ the system is equivalent to a Heisenberg antiferromagnet. In the undoped case, $W_+ = W_- = 1$ and the two terms in Eq. 39 contribute to the peak at $q = \pi$, one for $q \leq \pi$, the other for $q \geq \pi$ (cf. discussion below Eq. 27). In the fully doped case $W_+ = 4$, $W_- = 0$ and only the first term remains giving a peak at $q = 2\pi$. The fourfold increase in the amplitude W_+ that occurs when going from $c=0$ to $c=1$ is halved by the factor $(1 + c)^{-1}$ that appears as a prefactor in the expression for $\Phi(\kappa)$. Therefore, the area $\int_0^{2\pi} dq/(2\pi) \mathcal{S}(q)$, proportional to the number of spins per unit cell, just doubles as it must. As the hole concentration increases from $c = 0$ to $c = 0.5$ the peak shifts and the lineshape becomes increasingly different from that of the Heisenberg chain because the interval of momenta in which the presence of holes is relevant, $\Delta q \approx k_F$, gets bigger. Upon further increase of c the process reverts because k_F decreases back to zero (cf. the paragraph above Eq. 14).

The hypothesis of quasielastic scattering implicit in the preceding discussion is unlikely to be fulfilled under realistic experimental conditions. For $c \sim 0.3$, the excitation spectrum extends up to energies of the order of $E_F \sim 1 \text{ eV}$, whereas $\omega_N \lesssim 50 \text{ meV}$ in a typical spin-polarized neutron scattering experiment. An important reduction of intensity is thus expected to result from the fact that the excitation spectrum is only partially integrated. The peak intensity can be estimated by integrating Eq. 37 at $q = \pi(1 + c)$ up to ω_N , using Eq.

32. We find $d\sigma/d\Omega_s|_{max} \approx 60$ mbarn for $\omega_N \approx 50$ mev whereas, under the same conditions, Eq. 38 would predict $d\sigma/d\Omega_s|_{max} \approx 800$ mbarn. However, despite the large decrease of intensity, the predicted signal might still be observable in a high flux reactor.

We conclude by examining the expected finite-temperature corrections to the results obtained in this paper. The effects of temperature are different in the fermionic and spin subsystems. We show in Appendix C that the power-law behavior of the correlation function $\mathcal{C}_k(l; t = 0)$ that we found in Eq. 20, gives way to exponential decay at finite T :

$$\mathcal{C}_k(l; t = 0) = \exp\left(-\frac{k^2 l}{\pi \xi}\right), \quad (40)$$

where the typical scale of the correlations is $\xi = v_F/T$. The appearance of a finite decay length rounds-off the singularities of $C(q, \omega)$ at a scale $q \sim \xi^{-1}$, $\omega \sim T$. At room temperature $T \simeq 300$ K, and for $v_F \sim 1$ eV this should lead to a smearing of the peaks in Fig. 3 on a scale ~ 0.03 r.l.u., which is of the order of magnitude of the experimental resolution.

The changes in the spectral properties of the Heisenberg chain at finite T have been discussed by Müller et al. [16] who have shown that spectral weight appears below the bottom of the spin-wave continuum with increasing the temperature. At $k_B T/J = 0.5$, the total intensity in the region $\omega < \omega_s(k)$, is comparable to that at $\omega > \omega_s(k)$ but for $k_B T/J \simeq 0.1$ these effects are negligible and the correlation function is essentially identical to that at $T = 0$. For CuO chains where $J_{eff} \simeq 0.15$ eV and if the experiment is performed just above the superconducting transition temperature at $T \simeq 100$ K, the ratio is $T/J \simeq 0.1$. Under these conditions the predictions of our $T = 0$ calculations should remain valid.

ACKNOWLEDGMENTS

We thank V.P. Plakhty for useful discussions on the experimental aspects of this work. One of us (D.N.A.) acknowledges financial support from the Russian Foundation for Basic Research (Grant No. 96-02-18037-a) and a PECO fellowship from the French Ministère de la Recherche.

APPENDIX A: THE COHERENCE FACTOR

In this Appendix we derive the form of the coherence factor $A(Q, k)$ defined in Eq. 12. The Fourier components of the spin density are given by [18]

$$\mathbf{S}_Q = \sum_l e^{-iQl} (\mathbf{S}_l + e^{-iQ/2} \mathbf{S}_{l+1/2}) \equiv \mathbf{S}_Q|_{Cu} + \mathbf{S}_Q|_O, \quad (\text{A1})$$

where the right hand side of the equation defines the Cu and O contributions to \mathbf{S}_Q . Using the expansions 6 and 7 above and the identity $\hat{n} = (\exp ik\hat{n} - 1) / (\exp ik - 1)$ valid for any number operator \hat{n} and any value of k , the oxygen contribution may be cast in the form :

$$\mathbf{S}_Q|_O = (N + N_h)^{-1/2} \sum_k \boldsymbol{\sigma}_k \sum_l \exp i[(k - Q)(l + 1/2) + k\varphi(l)] \frac{\exp ik\hat{n}_{l+1/2} - 1}{2i \sin(k/2)}, \quad (\text{A2})$$

where $\varphi(l) = \sum_{j=0}^{l-1} \hat{n}_{j+1/2}$. Noticing that $\varphi(l) + \hat{n}_{l+1/2} = \varphi(l + 1)$ this is equivalent to

$$\mathbf{S}_Q|_O = (N + N_h)^{-1/2} \sum_k \boldsymbol{\sigma}_k \sum_l \exp i(k - Q)(l + 1/2) \frac{\exp ik\varphi(l + 1) - \exp ik\varphi(l)}{2i \sin(k/2)}. \quad (\text{A3})$$

Changing indices of summation from l to $l' = l + 1$ in the first summation in the equation above and recalling that periodic boundary conditions impose that $\varphi(N) - \varphi(0) = N_h$ and that $kN(1 + c) = 2\pi m_1$ and $QN = 2\pi m_2$ with m_1 and m_2 integers, we can rewrite Eq. A3 in the form

$$\mathbf{S}_Q|_O = (N + N_h)^{-1/2} \sum_k \boldsymbol{\sigma}_k \frac{\sin((Q - k)/2)}{\sin(k/2)} \sum_l \exp i[(k - Q)l + k\varphi(l)]. \quad (\text{A4})$$

Adding to this expression the trivial Cu contribution we get :

$$\mathbf{S}_Q = (N + N_h)^{-1/2} \sum_k \boldsymbol{\sigma}_k A(Q, k) \sum_l \exp i((k - Q)l + k\varphi(l)), \quad (\text{A5})$$

where we defined the coherence factor

$$A(Q, k) = 1 + \frac{\sin((Q - k)/2)}{\sin(k/2)}. \quad (\text{A6})$$

APPENDIX B: EVALUATION OF THE FERMIONIC CORRELATOR

The fermionic correlator is given by the expression

$$\langle \exp ik\mathcal{A}(l, t) \exp -ik\mathcal{A}(l', t') \rangle_{H_1}, \quad (\text{B1})$$

where the bosonic representation of $\mathcal{A}(l, t)$ has been given in Eq. 16 above. Eq. B1 may be easily evaluated by repeated application of the well-known formula

$$\exp(A + B) = \exp A \exp B \exp(-1/2[A, B]), \quad (\text{B2})$$

valid for any pair of operators A and B that satisfy $[A, [A, B]] = [B, [A, B]] = 0$.

We first use Eq. B2 in Eq. B1 in order to combine the two exponentials into one,

$$\begin{aligned} & \langle \exp ik\mathcal{A}(l, t) \exp -ik\mathcal{A}(l', t') \rangle_{H_1} = \\ & = \langle \exp ik \{ \mathcal{A}(l, t) - \mathcal{A}(l', t') \} \rangle_{H_1} \exp \left\{ \frac{k^2}{2} [\mathcal{A}(l, t), \mathcal{A}(l', t')] \right\}, \end{aligned} \quad (\text{B3})$$

where the commutator on the right hand side of Eq. B3 is a c -number given by (cf. Eq. 16) :

$$[A(l, t), A(l', t')] = -2i \sum_q v^2(q) \sin(v_F |q|(t - t')) \text{Re} [\phi(q, l) \phi(-q, l')]. \quad (\text{B4})$$

Next, we write $\mathcal{A}(l, t) - \mathcal{A}(l', t')$ as the difference of two bosonic operators,

$$\begin{aligned} \mathcal{A}(l, t) - \mathcal{A}(l', t') &= \mathcal{B}(l, l'; t, t') + \mathcal{B}^\dagger(l, l'; t, t'), \\ \mathcal{B}(l, l'; t, t') &= \sum_q v(q) \left(\phi(q, l) e^{-i\omega_q t} - \phi(q, l') e^{-i\omega_q t'} \right) b_{-q}. \end{aligned} \quad (\text{B5})$$

Using once more Eq. B2 we obtain :

$$\langle \exp ik(\mathcal{B} + \mathcal{B}^\dagger) \rangle = \exp -\frac{k^2}{2} [\mathcal{B}, \mathcal{B}^\dagger], \quad (\text{B6})$$

where

$$[\mathcal{B}, \mathcal{B}^\dagger] = 2 \sum_q v^2(q) \left\{ \frac{|\phi(q, l)|^2 + |\phi(q, m)|^2}{2} - \cos(v_F |q|t) \text{Re} [\phi(q, l) \phi(-q, m)] \right\}, \quad (\text{B7})$$

and we have used the fact that no bosons are excited in the ground-state. Combination of these results leads to the expression quoted in Eq. 18 of the main text.

APPENDIX C: TEMPERATURE DEPENDENCE OF THE FERMIONIC CORRELATOR

We show below that the correlation length of the fermion subsystem at finite temperature is $\xi = v_F/T$. For this we use a modification of an approach originally due to Lieb, Schultz and Mattis [20]. It is based on a representation of the instantaneous correlation function $\mathcal{C}_Q(l, 0; t = t')$ of Eq. 10 as the Toeplitz determinant

$$\begin{aligned}\mathcal{C}_Q(l) &= \langle \exp iQ \sum_q \Phi(q, l) \rho_q \rangle = \det(M) \\ M_{kl} &= \delta_{kl} - (1 - e^{iQ})g_{kl}.\end{aligned}\tag{C1}$$

The $l \times l$ matrix M is constructed out the fermionic correlation functions $g_{km} = \sin(\pi c(k - m))/\pi(k - m) = (1/2\pi) \int_{-\pi}^{\pi} dq n_q e^{iq(k-m)}$ where the Fermi function $n_q = 1/(1 + e^{\varepsilon_q/T})$. Notice that here we do not subtract the $q = 0$ component of the density in Eq. C1. Next, we use the asymptotic behavior of the above determinant at large l ,

$$\det(M) \sim \exp[lD - K_2],\tag{C2}$$

where [21]

$$D = iQ \int_{-\pi}^{\pi} \frac{dq}{2\pi} \tilde{n}_q,\tag{C3}$$

$$K_2 = Q^2 \int_{-\pi}^{\pi} \frac{dq dk}{2(2\pi)^2} \tilde{n}_q (1 - \tilde{n}_{q+k}) \frac{1 - \cos kl}{1 - \cos k},\tag{C4}$$

and $iQ\tilde{n}_q = \ln[1 - (1 - e^{iQ})n_q]$.

At $T = 0$ $\tilde{n}_q = n_q$ and we recover our results in the main text. For finite temperature, \tilde{n}_q is not so simple. For our purposes it is sufficient to expand \tilde{n}_q up to terms of order Q^2 :

$$iQ\tilde{n}_q = iQn_q - \frac{Q^2}{2}n_q(1 - n_q),\tag{C5}$$

from which the corrections to the two terms that appear in the exponent in Eq. C2 follow :

$$lD = iQcl - \frac{Q^2 l}{2\pi\xi},\tag{C6}$$

$$\begin{aligned}
K_2(T) - K_2(0) &= \frac{Q^2}{2\pi^2} \int_0^\pi \frac{dk}{k} \frac{1 - \cos kl}{\exp(kv_F/T) - 1} \\
&= \frac{Q^2}{2\pi^2} \ln \frac{\sinh \pi l/\xi}{\pi l/\xi}.
\end{aligned} \tag{C7}$$

Combining (C6) and (C7), one finds that at $Q \sim \pi$ and large l

$$|\mathcal{C}(l)| \sim \exp[-\pi l\xi]. \tag{C8}$$

REFERENCES

- [1] G.Uimin and J.Rossat-Mignod, *Physica C* **199**, 251 (1992).
- [2] H. A. Mook, P. Dai, K. Salama, D. Lee, F. Dogan, G. Aeppli, A. T. Boothroyd, and M.E. Mostoller, *Phys. Rev. Lett.* **77**, 370 (1996).
- [3] D. N. Bansov *et al.*, *Phys. Rev. Lett.* **74**, 598 (1995).
- [4] D.Hohlwein, in *Materials and Crystallographic Aspects of HT_c -Superconductivity*, edited by E.Kaldis (Kluwer Academic Publishers, Dordrecht, The Netherlands, 1994).
- [5] P.Schleger *et al.*, *Phys.Rev.Lett.* **74**, 1446 (1995).
- [6] J. Yu, S. Massida, A. J. Freeman, *Phys. Lett. A* **122**, 203 (1987).
- [7] W. E. Pickett, R. E. Cohen, and H. Krakauer, *Phys. Rev. B* **42**, 8764 (1990).
- [8] In an untwinned crystal this is the **b** crystalline axis. In practice, samples are twinned and only one-half of the magnetic intensity will be available along each of the **a** and **b** directions.
- [9] V.J.Emery, *Phys.Rev.Lett.* **58**, 2794 (1987).
- [10] P. Gawiec, D.R. Grempel, A.-C. Riiser, H. Haugerud, G. Uimin, *Phys.Rev.* **B 53**, 5872 (1996).
- [11] A.Krol, Z.H.Ming, Y.H.Kao, N.Nücker, G.Roth, J.Fink, G.C.Smith, K.T.Park, J.Yu, A.J.Freeman, A.Erband, G.Müller-Vogt, J.Karpinski, E.Kaldis, and K.Schönmann, *Phys.Rev.* **B 45** 2581 (1992).
- [12] P. Gawiec, D.R. Grempel, G. Uimin, and J. Zittartz, *Phys.Rev.* **B 53**, 5880 (1996).
- [13] A.I. Gogolin, A.S. Ioselevich, *JETP Lett.***53**, 375 (1991).
- [14] For finite U_d there are hopping processes in which the spin sequence changes but their amplitude, proportional to $t^2/(U_d - \epsilon_p)$, vanishes in the limit considered here.

- [15] A similar problem was discussed in J. Villain, and P. Bak, *J. Physique*, **42**, 657 (1981).
- [16] G. Müller, H. Thomas, H. Beck, J.C. Bonner, *Phys.Rev.* **B 24**, 1429 (1981).
- [17] A. Luther, I. Peshel, *Phys.Rev.* **B 12**, 3908 (1975).
- [18] We take the form factors of the Cu^{+2} an O^{-1} ions equal to unity, an excellent approximation in the domain of wavelength typical for magnetic neutron scattering.
- [19] D.C. Mattis, E.H. Lieb, *J. Math. Phys.* **6** , 304 (1965).
- [20] E. Lieb, T. Schultz, D. Mattis, *Ann. of Phys.* **16**, 407 (1961).
- [21] J.M. Luttinger, *J. Math. Phys.* **4** , 1154 (1963).
- [22] S.W.Lovesey, *Theory of Neutron scattering from Condensed Matter*, Oxford, Clarendon Press, 1988.

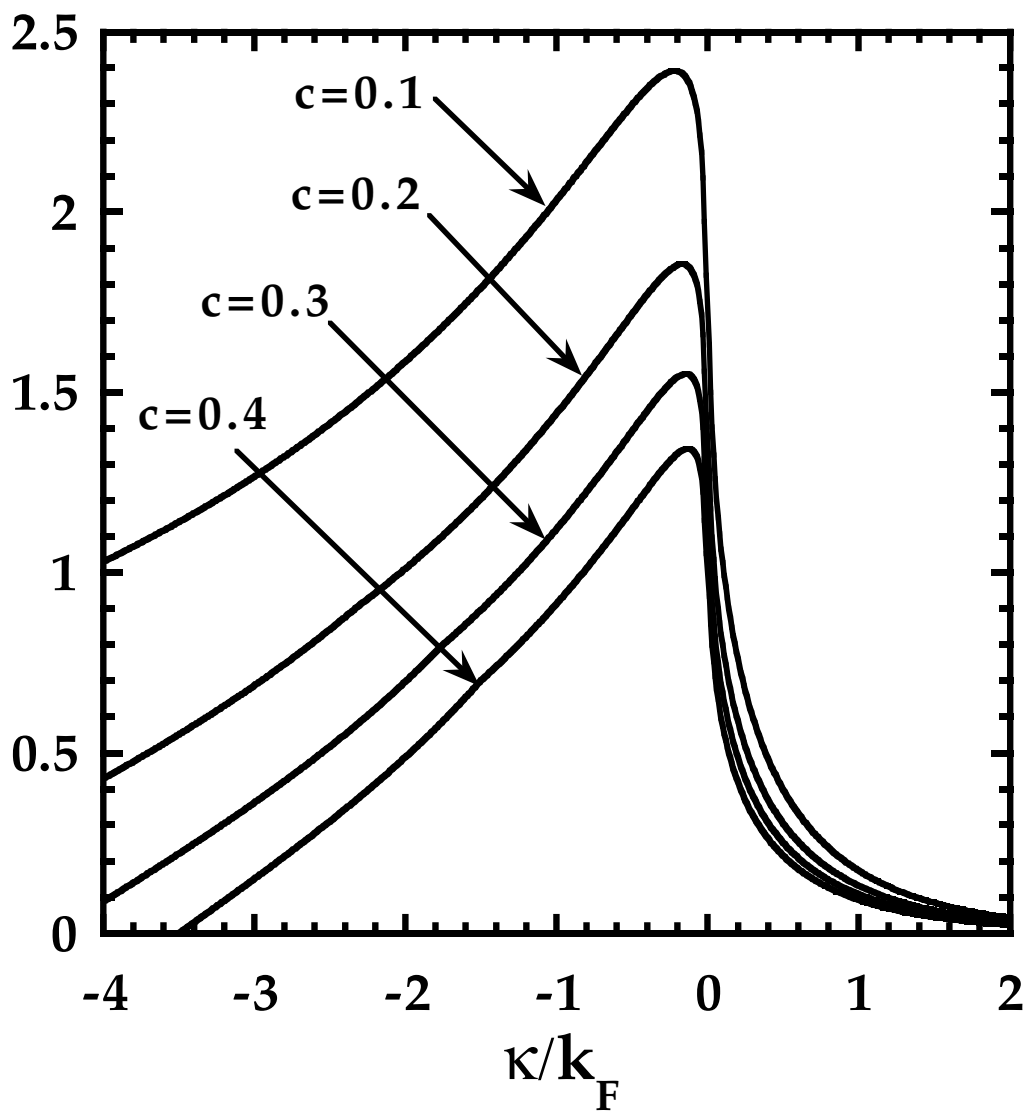
FIGURES

FIG. 1. The function $\Phi(\kappa)$ for the CuO chains for several values of the hole concentration c .

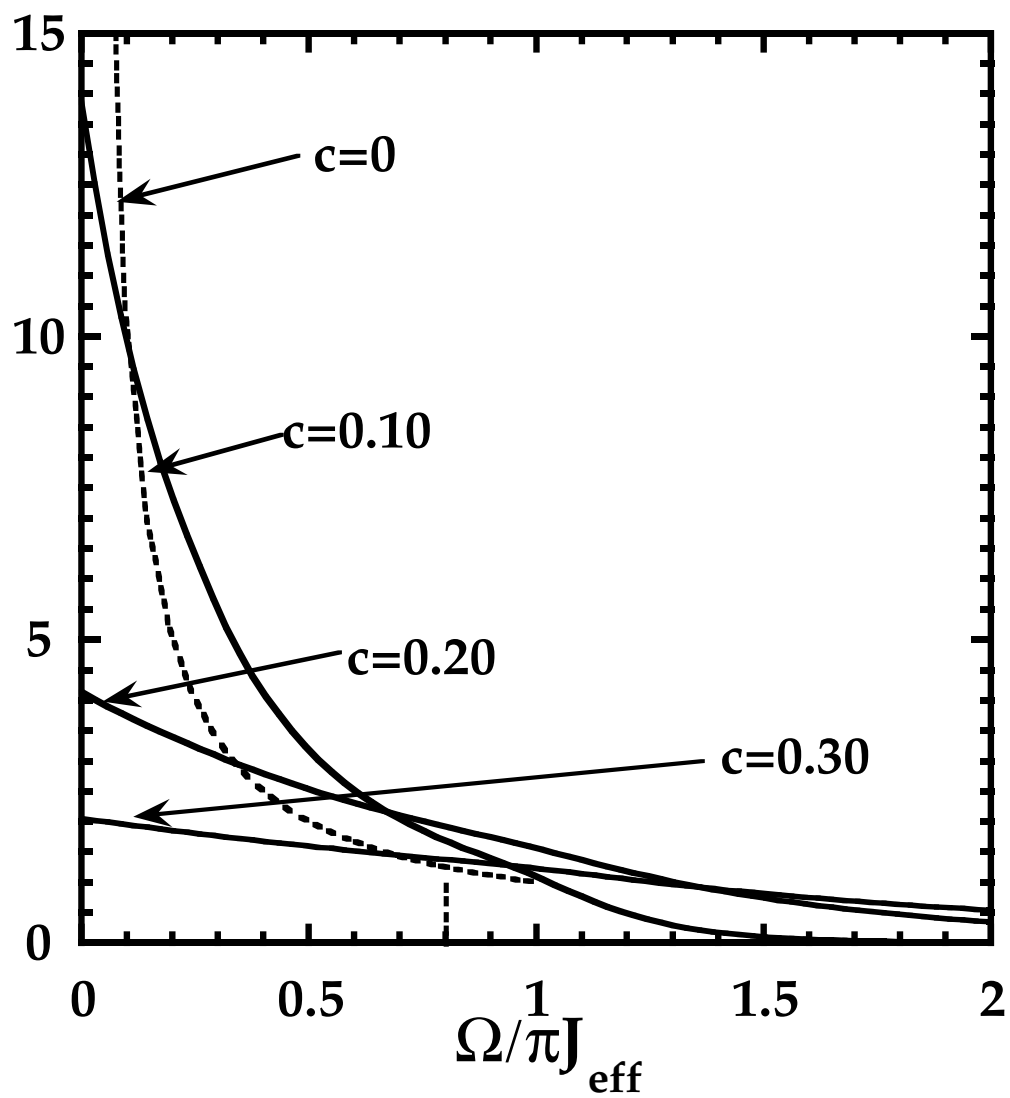
FIG. 2. Frequency dependence of $\Phi(0, \Omega)$ for three values of the hole concentration c . The ratio of the effective exchange constant to the hole hopping integral is $J_{eff}/\tau = 1/3$.

FIG. 3. Equal-time spin-spin correlation of the CuO chains as function of q and of the hole concentration c .

$\Phi(\kappa)$



$$2\pi J_{\text{eff}} \Phi(0, \Omega)$$



$S(q)$

